ACTA CHEMICA SCANDINAVICA 25 (1971) 866–876

The Significance of π Back-bonding in Compounds with Pyrite, Marcasite, and Arsenopyrite Type Structures

A. KJEKSHUS and D. G. NICHOLSON*

Kjemisk Institutt A, Universitetet i Oslo, Blindern, Oslo 3, Norway

The structural data on compounds with the pyrite, marcasite, and arsenopyrite type crystal structures have been examined and are found to give no indication of π back-bonding between the metal and non-metal atoms. The same conclusion is reached on reexamining the Mössbauer parameters for the iron dichalcogenides and dipnictides.

The structural, electrical, and magnetic properties of binary and some ternary compounds with the FeS_2-*p* (*p* = pyrite), FeS_2-*m* (*m* = marcasite), and $CoSb_2$ (FeAsS-arsenopyrite) type crystal structures have, during the past five years, been extensively studied at this Institute.[1–16] Although a bonding scheme for these substances has been proposed [17,18] which accounts reasonably well for experimental observations, the significance of π interactions between the metal and non-metal atoms has not been thoroughly examined. However, from the symmetry of these structure types, π back-bonding is allowed, and this possibility should indeed be considered. Additional information concerning the bonding in these compounds is contained in the variations of the observed bond lengths and the ^{57}Fe Mössbauer parameters for the compounds containing iron.

BOND LENGTHS

A common feature of the three structure types under consideration is that they contain bonding $T-X$ and $X-X$ distances, where T and X designate metal and non-metal atoms, respectively. (The $CoSb_2$ type has also additional bonding $T-T$ distances, which will not be discussed here.) As a consequence of the bonding $X-X$ distance (which in the previous bond considerations [17,18] was assumed to represent a single bond) there is an internal measure for the

* Postdoctorate fellow, Royal Norwegian Council for Scientific and Industrial Research.

radius * of the X atom (r_X) built into the crystal structure. Since r_X is one of the factors governing the $T-X$ bond length, it will be useful to investigate the relationship between the $X-X$ and $T-X$ bond distances. The other factor influencing the $T-X$ bond length is the radius of T (r_T).

As shown in Fig. 1 there is a distinct correlation between the two categories of interatomic distances. A conspicuous feature of this figure is the linear relationship between the bonding $X-X$ and $T-X$ distances for a given T while varying X within a Group of the Periodic System. It should be noted that the observed $X-X$ and $T-X$ distances are not independent parameters, since they are interrelated through the positional coordinates and the unit cell dimensions. The simplest interpretation for the linear trend in Fig. 1 is that r_T remains approximately constant in a series of compounds, or, alternatively r_T is itself a linear function of r_X. (The scale of the diagram is such that variations in r_T of the order of a few hundredths of an Ångström will not be noticeable.) An examination of the data for the manganese dichalcogenides (where a good linear fit is obtained in Fig. 1), for example, shows that r_T varies very slowly, but approximately linearly with r_X. The actual values for r_X; r_T are 1.04_5; 1.54_7, 1.16_5; 1.54_4, and 1.37_5; 1.53_2 Å for MnS_2, $MnSe_2$, and $MnTe_2$, respectively. This tendency for a decrease in r_T with increasing atomic number of X is a common feature for most of the series, the implications of which are discussed further on.

As seen from Fig. 1 there are some deviations from linearity which require an explanation. In the construction of the diagram, all binary compounds for which positional coordinates are available have been included, and it would not be unexpected, therefore, if experimental errors are a cause of some of these discrepancies. This is a possibility for $FeAs_2$, RuP_2, $RuAs_2$, OsP_2, RhP_2, and IrP_2,[8,16] and it would be of interest to have these structures redetermined on the basis of single crystal data.

A comparison of the data [10,13] for the pyrite and marcasite modifications of FeS_2 shows that there is a marked change in both r_X and r_T (Fig. 1), but since only series of isostructural compounds are relevant to the discussion this does not represent a real discrepancy.

It is apparent from Fig. 1 that the reported variation in composition for the metal deficient FeS_2-p type structures of the rhodium and iridium chalcogenides (*cf.* Refs. 19–21) is of subordinate importance in influencing r_X and r_T.

Other factors which could produce a departure from linearity in Fig. 1 are (a) variations in the electronic band structure, (b) changes in the number of localized unpaired electrons on T, (c) a varying degree of ionicity, and (d) a variation in the degree of π back-bonding between T and X. Point (a) is apparently relevant only when comparing cases like $PdAs_2$ and $PdSb_2$ with $PtAs_2$ and $PtSb_2$ (metallic type of conduction *versus* semiconduction, *cf.* Ref. 22), point (b) is probably of importance when considering NiS_2 and $NiSe_2$

* The term "radius" is here used loosely as a measure of atomic size. However, this appears to be a reasonable approximation within this family of structures, where distortion and bond strength are interrelated. Furthermore, the implication of spherical symmetry through this description has no effect on the conclusions.

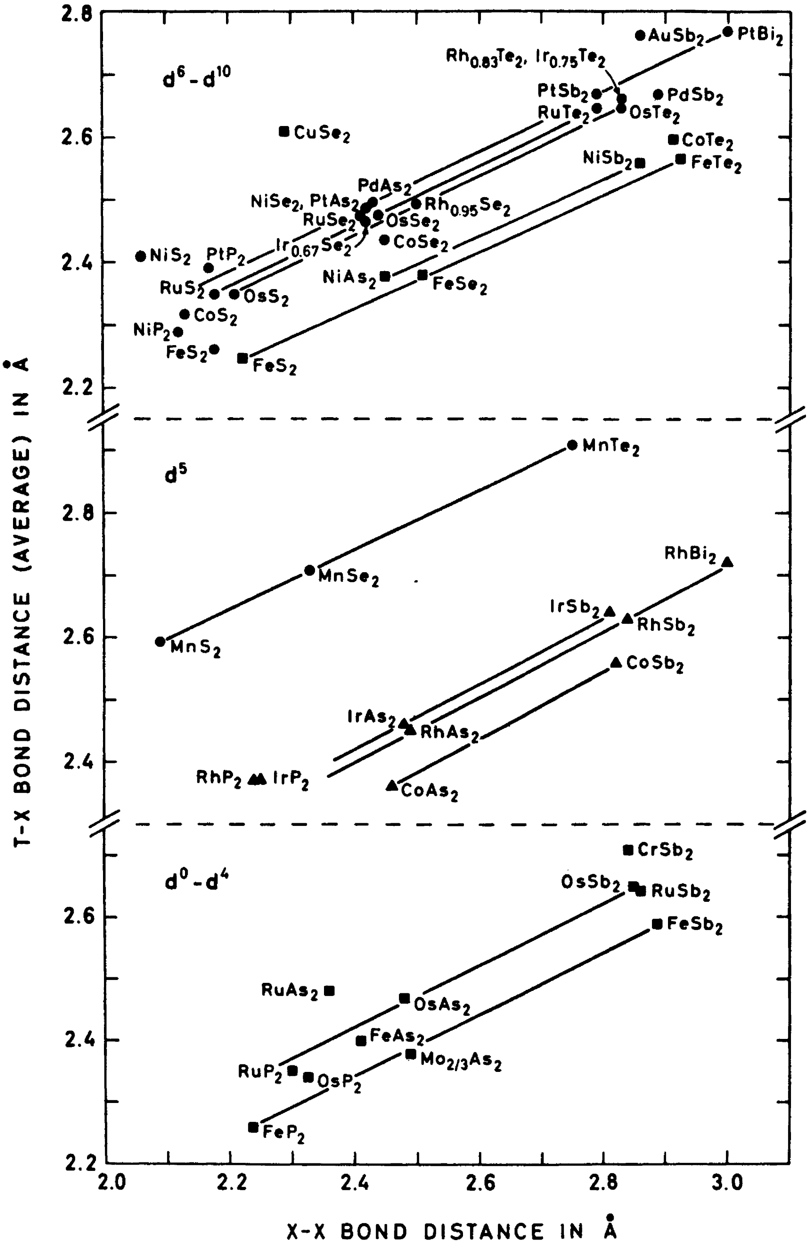

Fig. 1. $X-X$ *versus* (average) $T-X$ bond distance for compounds with the FeS_2-*p* (●), FeS_2-*m* (■), and $CoSb_3$ (▲) type crystal structures. The straight lines connect isostructural compounds with a common metal atom.

(two unpaired electrons per Ni atom *versus* a delocalized electron configuration, *cf.*, *e.g.*, Ref. 11), and for point (c) there seems to be no reliable measure.

On considering the final point, which is the object of the study, it is relevant to point out that not only does the figure demonstrate linear relationships, but it shows that the lines are also approximately parallel. The data for the manganese dichalcogenides may be taken as a reference. The magnetic susceptibility and neutron diffraction data [23] confirm that Mn has a high-spin d^5 configuration in this series, which immediately eliminates the possibility of a significant degree of π back-bonding between Mn and chalcogen. Since the other series of compounds in Fig. 1 exhibit a parallel relationship with the manganese dichalcogenides, their bonding must be predominantly of a similar nature,

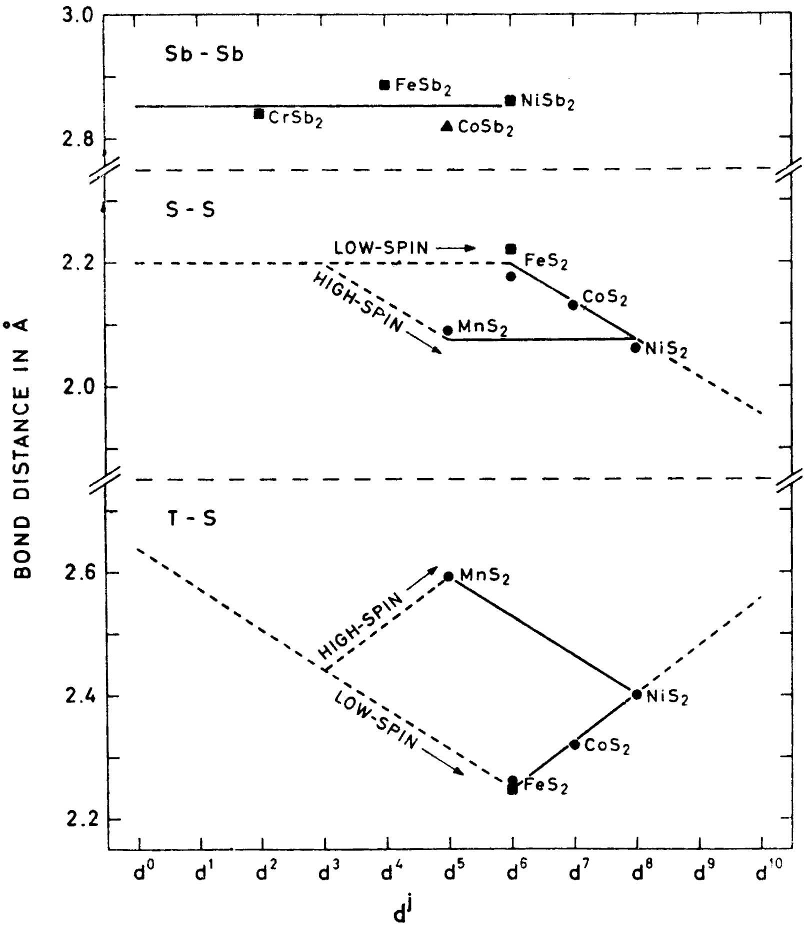

Fig. 2. Bond distances as a function of d^j configuration. The symbols used to distinguish between the different structure types correspond with those in Fig. 1.

and $T-X$ π back-bonding should therefore be relatively insignificant in all these compounds. Furthermore, the degree of $T-X$ π back-bonding is expected to decrease as the atomic number of X increases within a series. This is contrary to the observed decrease in r_T with increasing atomic number of X in most of the series.

The variation of the $T-X$ bond length with the electron configuration (d^j) localized on T for the disulphides of the $3d$ metals is illustrated in the bottom part of Fig. 2. (The particular choice of these compounds is motivated by the fact that their magnetic data unambiguously support the assigned d^j configuration; *cf.* Ref. 18.) The full lines connect the observed points, while the broken lines (which are, in this diagram, experimentally unfounded) are drawn parallel to the full lines. The resulting figure is similar to that due to Pearson [24] for the radius of the "divalent" $3d$ metals in octahedral coordination as a function of d^j configuration. (Such diagrams reflect a small portion of the atomic size *versus* atomic number relationship for the elements, as frequently shown in textbooks.)

The $T-X$ bond length, for a given X atom, is a function of r_T as well as the bond strength of the $T-X$ bond. The changes in r_T, however, outweigh the differences in bond strength in this case, and the bottom part of Fig. 2 is therefore essentially a diagram of the variation in r_T with the d^j configuration. The broken line from d^0 to low-spin d^6 reflects the decrease in r_T on progressively increasing the atomic number of T and the number of electrons contained in essentially non-bonding t_{2g} bands. The increased $T-S$ bond length at MnS_2 is due to the high-spin d^5 configuration of Mn, where two electrons enter anti-bonding e_g* bands. Similarly, the steady increase in $T-S$ from low-spin d^6, through low-spin d^7 to d^8 results from an increasing number of electrons entering the anti-bonding e_g* bands. The full line from MnS_2 to NiS_2 runs through hypothetical high-spin compounds.

Although it is evident that the dependences of r_T on d^j configuration mask the variations in $T-X$ bond strengths, information on these are contained in the corresponding $X-X$ bond lengths. The change in the $S-S$ bond length with the d^j configuration of T is also shown in Fig. 2. The shortest $S-S$ distances are found for MnS_2 and NiS_2 and the longest for FeS_2; a steady decrease is seen on going from FeS_2 through CoS_2 to NiS_2. The parallelogram in the middle section of Fig. 2 is constructed by drawing the broken lines parallel to the experimentally founded, full lines. The horizontal line from d^0 to low-spin d^6 in this diagram is supported by the dependence of the $Sb-Sb$ bond lengths on d^j configuration for the corresponding diantimonides shown in the top part of Fig. 2.

An approximately constant $X-X$ bond length (for a given X) for d^0 to low-spin d^6 configurations of T implies that the $T-X$ bond strengths are similar in such compounds. This is consistent with the view [18] that the additional electrons which enter t_{2g} bands must be virtually non-bonding. Accepting that the bonding in these compounds is of a predominantly covalent nature (*vide infra*), the $X-X$ bond lengths in the interval d^0 – low-spin d^6 are longer than the corresponding single bond lengths listed by, *e.g.*, Pauling.[25] This may be accounted for by noting that the bonding interaction between the X and T atoms will result in some depletion of the electron density on the

$X-X$ pairs. Since the density of bonding electrons is concentrated between the nuclei concerned, any depletion in this electron density is equivalent to a decrease in bond strength. In inorganic macromolecules of the type considered here, an increase in the $T-X$ bond strength consequently results in a decrease in the strength of the $X-X$ bond.

When the t_{2g} bands are filled, the additional electrons go into the anti-bonding $e_g{}^*$ bands. The presence of anti-bonding electrons weakens the $T-X$ bond and causes a consequent increase in $X-X$ bond strength. For the disulphides considered in Fig. 2, the progressive decrease in S–S bond lengths with an increase in the population of the anti-bonding $e_g{}^*$ bands clearly demonstrates that the S–S bond strength depends on the number of electrons contained in these bands. The order for the S–S bond strengths in these compounds is $NiS_2 \sim MnS_2 > CoS_2 > FeS_2$. (The difference between the pyrite and marcasite modifications of FeS_2 emphasizes the modifying influence of the structure type on bond strength.) According to this scheme, the shortest $X-X$ bond lengths are to be found in compounds where T has a d^{10} configuration. This prediction can be tested when the positional parameters become available for the recently discovered [26] zinc dichalcogenides with the FeS_2-p type structure.

Elliott [27] was the first to correlate the variations in the interatomic $T-$S and S–S distances for disulphides with the FeS_2-p type structure with the d^j configuration of T. However, since he uses an ionic model and crystal field theory, his interpretation differs substantially from that presented above. An ionic model is, on the other hand, clearly inconsistent with the Mössbauer parameters for the iron dichalcogenides and dipnictides.

From the structural data it is concluded that there is no evidence for π back-bonding by the participation of the t_{2g} electrons of T and these remain essentially non-bonding. The variations in $X-X$ and (in part) $T-X$ bond lengths with the d^j configuration of T (for a given X) is attributed to the changes in bond strength on populating the anti-bonding $e_g{}^*$ bands.

REEXAMINATION OF MÖSSBAUER DATA

Mössbauer chemical shifts (δ) and quadrupole splittings (Δ) for the dichalcogenides and dipnictides of iron have been collected from various references, and are listed in Table 1. Some of the values have also been confirmed by the present authors. With a few exceptions the various data for each compound are in reasonable agreement.

The Mössbauer chemical shifts for the iron dichalcogenides (in contrast to the dipnictides) have previously been interpreted [28,36] by invoking a significant degree of π back-bonding. Since such an interpretation is inconsistent with the overall picture presented in the preceding section, the Mössbauer data should be subjected to a reexamination.

The Mössbauer chemical shift depends on the total s electron density at the nucleus, whereas the occupation of d and p orbitals influence δ indirectly by virtue of their shielding properties.

The values of δ listed in Table 1 must be taken as a clear evidence for the covalent nature of the compounds. Attempts have, nevertheless, been made [28,36]

Table 1. Mössbauer parameters (^{57}Fe) for the dichalcogenides and dipnictides of iron. (Chemical shifts are given with respect to metallic iron. Error limits are bracketed after the corresponding values.)

Compound	Structure type	T (°K)	δ (mm/s)	Δ (mm/s)	Reference quoted	Further references
FeS_2	FeS_2-*p*	300	0.314(2)	0.614(6)	28	29 – 33 [d]
	FeS_2-*p*	81	0.407(3)	0.620(9)	28	30, 31
	FeS_2-*p*	300, 50 kbar	0.23 [a]	0.77 [a]	32	
	FeS_2-*m*	300	0.277(2)	0.506(7)	28	29, 30, 33 [d]
	FeS_2-*m*	81	0.373(2)	0.504(6)	28	30
$FeSe_2$	FeS_2-*m*	300	0.395(4)	0.584(10)	28	
	FeS_2-*m*	81	0.493(5)	0.566(10)	28	
$FeTe_2$	FeS_2-*m*	300	0.471(5)	0.502(11)	28	[d]
	FeS_2-*m*	81	0.577(6)	0.524(10)	28	
FeP_2	FeS_2-*m*	300	0.09(3)	2.08(2)	34	35 [d]
	FeS_2-*m*	80	0.07(2)	2.06(2)	34	
	?	R.t., h.p. [b]	0.32	~ 0 [c]	35	
$FeAs_2$	FeS_2-*m*	293	0.39(2)	1.68(7)	31	35 [d]
	FeS_2-*m*	77	0.39(2)	1.71(7)	31	
	?	R.t., h.p. [b]	0.28	~ 0 [c]	35	
$FeSb_2$	FeS_2-*m*	300	0.455(4)	1.281(16)	28	35 [d]
	FeS_2-*m*	81	0.569(5)	1.585(19)	28	
	?	R.t., h.p. [b]	0.31	~ 0 [c]	35	
FeAsS	$CoSb_2$	293	0.34(2)	1.05(5)	31	
	$CoSb_2$	77	0.35(2)	1.07(5)	31	

[a] Estimated from a diagram. [b] Room temperature, high pressure. [c] Not observed. [d] Present article.

to correlate these data with the "oxidation state" groupings, proposed by Walker *et al.*,[37] on the basis of essentially ionic reference compounds. (A number of similar relationships between δ and the electron configuration of iron are found in the literature, which differ mainly in the assumptions made, concerning the selected reference compounds.) The correlation diagram of Walker *et al.* has proved to be unsatisfactory in a number of cases, and some of the discrepancies have been attributed to the perturbation of the 3*d* shell of iron by the chemical bonding.[38] The δ values for covalent iron compounds are, in fact, somewhat insensitive to differences in the formal oxidation state.

The values of δ for the iron dichalcogenides (Table 1) are quite low in comparison with those for Fe^{2+} salts, whereas they are generally much higher than those for covalent (low-spin) Fe(II) compounds, where π back-bonding is supposed to be significant (*cf.*, *e.g.*, Ref. 38). The δ values for the iron dipnictides are slightly lower than those for the corresponding dichalcogenides. This can be attributed, in part, to the increased shielding by the two additional non-bonding t_{2g} electrons on Fe in the latter compounds. The low δ values for the iron dichalcogenides and dipnictides may reflect an increased 4*s* and/or a decreased 3*d* and 4*p* character of the bonding σ bands. Both effects would lead to a relative increase in the *s* electron density at Fe. The progressive increase in δ within both series of compounds shows that the effective *s* electron density at Fe decreases as the atomic number of X increases. This may be taken as evidence for a (slight) decrease in Fe – X bond strength with increasing atomic number of X, *i.e.* consistent with a corresponding decrease in the donor ability of X.

There is a significant difference in δ between the two modifications of FeS_2 (Table 1), which suggests that the Fe – S bonds in the marcasite form are slightly stronger than in pyrite. This view is consistent with the shorter average Fe – S bond length in the marcasite modification and shows the importance of the structure type on bond strength.

The Mössbauer quadrupole splitting is a measure of the asymmetry of the total wave function at the iron nucleus, and this parameter can be useful in examining the σ donor and possible π acceptor properties of the atoms bonded to iron. The effect on Δ by a π component would be opposite in sign to that produced by the σ component. The increase in electron asymmetry at the iron nucleus produced by removing two t_{2g} electrons on going from the dichalcogenides to the dipnictides results in larger Δ values for the latter compounds. This is in addition to the differences in electron asymmetry caused by the different bonding characteristics of the chalcogen and pnigogen atoms.

The quadrupole interactions for the iron dichalcogenides are a result of an imbalance in the distribution of the d (and p) electrons caused by a distortion of the X_6 octahedra around Fe. Δ does not vary uniformly with the atomic number of the chalcogen, but reaches an apparent maximum with $FeSe_2$. In the dipnictide series, on the other hand, Δ undergoes a progressive decrease with increasing atomic number of the pnigogen. The fact that the crystallographically more symmetric pyrite modification of FeS_2 has a larger Δ value than marcasite strongly suggests that it is the latter modification which departs from the trend in having an anomalously low Δ value. The crucial difference between FeS_2-*m* and FeP_2 is, in this context, the presence of a filled (say) d_{xy} orbital in the former, which is directed along [001] of the unit cell and points towards a similar orbital from a neighbouring iron atom (see Ref. 18). The smaller size of the sulphur atom allows a closer approach of the lobes of the d_{xy} orbital in the structure of FeS_2-*m* than in the corresponding modifications of $FeSe_2$ and $FeTe_2$. The interaction of the d_{xy} orbital on neighbouring iron atoms raises it in energy relative to the d_{yz} and d_{zx} orbitals and may, moreover, cause a reduction in the imbalance of the overall electron density on iron. This perturbation diminishes with increasing size of the chalcogen atom and it is absent in the dipnictide series.

The asymmetry in the electron distribution around the iron nucleus may perhaps be divided into two categories, one which is associated with the bonding orbitals, and one which is due to any distortion of the non-bonding t_{2g} orbitals. The latter component may either be a result of distortion, as in the iron dichalcogenides, or be predominantly due to an electron imbalance, as in the case of the iron dipnictides.

Since the repulsive interation between the d_{xy} orbitals on neighbouring Fe atoms reaches a maximum at FeS_2-*m*, it may be suggested that the two above effects oppose each other in the dichalcogenide series. The electric field gradient at the Fe nucleus produced by the filled d_{xy} orbital can be regarded [39] as being proportional to $+{}^4/_7\langle r^{-3}\rangle k_1$ (where the factor k_1 is a measure of the distortion relative to an undistorted d_{xy} orbital). The d_{yz} and d_{zx} orbitals are less distorted and very similar in energy (if not degenerate). The electric field gradients due to the latter orbitals are proportional to $-{}^2/_7\langle r^{-3}\rangle k_2$ and $-{}^2/_7\langle r^{-3}\rangle k_3$ (where the factors k_2 and k_3 become equal in the case of degeneracy). The total electric field gradient due to the t_{2g} orbitals is hence $-{}^{2}/_{7}\langle r^{-3}\rangle(k_2+k_3-2k_1)$. In the case of the more crystallographically symmetric FeS_2-*p* it seems reasonable to assume that the term $(k_2+k_3-2k_1)$ approaches zero, and that the Δ value of 0.614(6) mm/s at 300°K therefore reflects predominantly the asymmetry of the bonding orbitals. The decreased Δ value for FeS_2-*m* accordingly suggests that $2|k_1|>|k_2+k_3|$, which is consistent with the increased energy of the d_{xy} orbitals (*vide supra*). The term $(k_2+k_3-2k_1)$ clearly decreases in the sequence $FeS_2-FeSe_2-FeTe_2$. In the case of the iron dipnictides, the electric field gradient due to the filled d_{yz} and d_{zx} orbitals is proportional to $-{}^{2}/_{7}\langle r^{-3}\rangle(k_2'+k_3')$. This term is opposite in sign to the corresponding one for the iron dichalcogenides. For the iron dipnictides, the contributions to the electric field gradient at the iron nucleus from the bonding orbitals and the non-bonding t_{2g} orbitals are of the same sign. This appears to account for the relatively large Δ values for the iron dipnictides.

If π back-bonding is a significant factor in the $Fe-X$ bonding, then a progressive increase in Δ with increasing atomic number of X would be expected. This is opposite to the trend found in Table 1, which shows that the order for the Δ values is $FeP_2>FeAs_2>FeSb_2$ and (neglecting FeS_2, *vide supra*) $FeSe_2>FeTe_2$.

$FeSb_2$ shows an anomalously large increase in Δ between 81 and 300°K (Table 1), which may result from a thermal population of the d_{xy} orbital from the filled (at absolute zero) d_{yz} and d_{zx} orbitals (*cf.* Refs. 18, 28). (A similar phenomenon does not occur in FeP_2 or $FeAs_2$, where the $Fe-Fe$ distances along [001] are shorter than in $FeSb_2$, and hence the energy separation between d_{xy} on the one hand, and d_{yz} and d_{zx} on the other become larger.) The same explanation has been offered [14,18] for the anomalous temperature dependence of the magnetic susceptibility curve for this compound. (Neutron diffraction data collected between 4 and 300°K confirm that no cooperative magnetic phenomenon occurs within this region.[14] Furthermore, $FeSb_2$ does not undergo a structural transformation below room temperature.) More data are, however, needed in order to confirm this suggestion.

High pressure Mössbauer data are available for FeS_2-*p*, FeP_2, $FeAs_2$, and $FeSb_2$ (Table 1). The decrease in δ generally observed on the application of high pressure is a reflection of the compression of the *s* electron wave functions, and the decreased shielding caused by the "spreading out" of the iron 3*d* electrons because of the increased orbital overlap.[40] In the case of FeP_2, δ increases on the application of high pressure, but it is difficult to propose a non-speculative interpretation for this phenomenon.

The effect of high pressure on Δ is different for FeS_2-*p* on the one hand, and the iron dipnictides on the other. The progressive increase in Δ with increasing pressure, which is observed for FeS_2-*p*, is associated with an increasing electronic distortion. High pressures induce a large decrease in Δ for the iron dipnictides, and this may be due to a decrease in *d* electron imbalance produced by a redistribution of electron density as a consequence of the altered t_{2g} band structure. Further discussion on this effect must await results from similar experiments on the marcasite modifications of the iron dichalcogenides.

In addition to the ^{57}Fe Mössbauer data, considered above, a recent paper [41] has been published concerning the ^{125}Te Mössbauer effect in $MnTe_2$. However, in view of the lack of suitable reference compounds, the bonding implications of these data are difficult to assess at present. It should nevertheless be mentioned that Pasternak and Spijkervet [41] interpreted their data in terms of a purely ionic model which is clearly incorrect.

Within the family of compounds under consideration, the Mössbauer effect can be observed for those containing the following elements: Ni, Zn, Ru, Os, Ir, Pt, Au, and Sb in addition to Fe and Te. When data for those compounds containing the additional Mössbauer nucleides become available, there will be more detailed bonding information at hand.

CONCLUSION

All the properties of compounds with the FeS_2-*p*, FeS_2-*m*, and $CoSb_2$ type crystal structures suggest that the bonding is of a highly covalent nature, and this is confirmed by the Mössbauer data for the iron dichalcogenides and dipnictides. Neither the structural, nor the Mössbauer data give any indication for the need to invoke π back-bonding from the essentially non-bonding t_{2g} orbitals on the metal to the non-metal atoms.

A survey of the literature suggests that, perhaps, the importance of π back-bonding has, in general, been over-emphasized, particularly in relation to Mössbauer spectroscopy. It is therefore considered relevant to draw attention to a recent paper by Venanzi [42] who points out that π bonds need not always be invoked just because they are allowed by symmetry.

Acknowledgement. One of the authors (D. G. N.) expresses his appreciation to the *Royal Norwegian Council for Scientific and Industrial Research* for the grant of a post-doctorate fellowship.

REFERENCES

1. Furuseth, S., Selte, K. and Kjekshus, A. *Acta Chem. Scand.* **19** (1965) 735.
2. Fermor, J. H. and Kjekshus, A. *Rev. Sci. Instr.* **36** (1965) 763.
3. Furuseth, S. and Kjekshus, A. *Acta Chem. Scand.* **19** (1965) 1405.
4. Furuseth, S., Selte, K. and Kjekshus, A. *Acta Chem. Scand.* **21** (1967) 527.
5. Fermor, J. H., Furuseth, S. and Kjekshus, A. *J. Less-Common Metals* **11** (1966) 376.
6. Andresen, A. F., Furuseth, S. and Kjekshus, A. *Acta Chem. Scand.* **21** (1967) 833.
7. Holseth, H. and Kjekshus, A. *Acta Chem. Scand.* **22** (1968) 3273.
8. Holseth, H. and Kjekshus, A. *Acta Chem. Scand.* **22** (1968) 3284.
9. Holseth, H. and Kjekshus, A. *J. Less-Common Metals* **16** (1968) 472.
10. Brostigen, G. and Kjekshus, A. *Acta Chem. Scand.* **23** (1969) 2186.
11. Furuseth, S., Kjekshus, A. and Andresen, A. F. *Acta Chem. Scand.* **23** (1969) 2325.
12. Holseth, H. and Kjekshus, A. *Acta Chem. Scand.* **23** (1969) 3043.
13. Brostigen, G. and Kjekshus, A. *Acta Chem. Scand.* **24** (1970) 1925.
14. Holseth, H., Kjekshus, A. and Andresen, A. F. *Acta Chem. Scand.* **24** (1970) 3309.
15. Bjerkelund, E. and Kjekshus, A. *Acta Chem. Scand.* **24** (1970) 3317.
16. Kjekshus, A. *Acta Chem. Scand.* **25** (1971) 411.
17. Brostigen, G. and Kjekshus, A. *Acta Chem. Scand.* **24** (1970) 2983.
18. Brostigen, G. and Kjekshus, A. *Acta Chem. Scand.* **24** (1970) 2993.
19. Haraldsen, H. *Experientia Suppl.* **7** (1957) 165.
20. Hulliger, F. *Nature* **204** (1964) 644.
21. Parthé, E., Hohnke, D. and Hulliger, F. *Acta Cryst.* **23** (1967) 832.
22. Hulliger, F. *Nature* **200** (1963) 1064.
23. Hastings, J. M., Elliott, N. and Corliss, L. M. *Phys. Rev.* **115** (1959) 13.
24. Pearson, W. B. *Z. Krist.* **126** (1968) 362.
25. Pauling, L. *The Nature of the Chemical Bond*, Cornell University Press, Ithaca 1960.

26. Bither, T. A., Bouchard, R. J., Cloud, W. H., Donohue, P. C. and Siemons, W. J. *Inorg. Chem.* **7** (1968) 2208.
27. Elliott, N. *J. Chem. Phys.* **33** (1960) 903.
28. Temperley, A. A. and Lefévre, H. W. *J. Phys. Chem. Solids* **27** (1966) 85.
29. Solomon, I. *Compt. Rend.* **250** (1960) 3828.
30. Kerler, W., Neuwirth, W., Fluck, E., Kuhn, P. and Zimmermann, B. *Z. Physik* **173** (1963) 321.
31. Imbert, P., Gérard, A. and Wintenberger, M. *Compt. Rend.* **256** (1963) 4391.
32. Vaughan, R. W. and Drickamer, H. G. *J. Chem. Phys.* **47** (1967) 468.
33. Morice, J. A., Rees, L. V. C. and Rickard, D. T. *J. Inorg. Nucl. Chem.* **31** (1969) 3797.
34. Rundqvist, S., Wäppling, R. and Karlsson, E. *Second International Conference on Solid Compounds of Transition Elements*, Enschede 1967, p. 122.
35. Kasper, H. and Drickamer, H. G. *Proc. Natl. Acad. Sci. U.S.* **60** (1968) 773.
36. Kerler, W., Neuwirth, W. and Fluck, E. *Z. Physik* **175** (1963) 200.
37. Walker, L. R., Wertheim, G. K. and Jaccarino, V. *Phys. Rev. Letters* **6** (1961) 98.
38. Danon, J. In Goldanskii, V. I. and Herber, R. H. *Chemical Applications of Mössbauer Spectroscopy*, Chapter 3, Academic, New York – London 1968.
39. Ingalls, R. *Phys. Rev.* **A 133** (1964) 787.
40. Ingalls, R., Coston, C. J., De Pasquali, G. and Drickamer, H. G. *J. Chem. Phys.* **45** (1966) 1057.
41. Pasternak, M. and Spijkervet, A. L. *Phys. Rev.* **181** (1969) 574.
42. Venanzi, L. M. *Chem. Brit.* **1968** **162.**

Received June 30, 1970.